

# Attribute-Guided Face Generation Using Conditional CycleGAN

Yongyi Lu<sup>1</sup>[0000-0003-1398-9965], Yu-Wing Tai<sup>2</sup>[0000-0002-3148-0380], and  
Chi-Keung Tang<sup>1</sup>[0000-0001-6495-3685]

<sup>1</sup> The Hong Kong University of Science and Technology

<sup>2</sup> Tencent Youtu

{yluaw, cktang}@cse.ust.hk, yuwingtai@tencent.com

**Abstract.** We are interested in attribute-guided face generation: given a low-res face input image, an attribute vector that can be extracted from a high-res image (attribute image), our new method generates a high-res face image for the low-res input that satisfies the given attributes. To address this problem, we condition the CycleGAN and propose conditional CycleGAN, which is designed to 1) handle unpaired training data because the training low/high-res and high-res attribute images may not necessarily align with each other, and to 2) allow easy control of the appearance of the generated face via the input attributes. We demonstrate high-quality results on the *attribute-guided conditional CycleGAN*, which can synthesize realistic face images with appearance easily controlled by user-supplied attributes (e.g., gender, makeup, hair color, eyeglasses). Using the attribute image as identity to produce the corresponding conditional vector and by incorporating a face verification network, the attribute-guided network becomes the *identity-guided conditional CycleGAN* which produces high-quality and interesting results on identity transfer. We demonstrate three applications on identity-guided conditional CycleGAN: identity-preserving face superresolution, face swapping, and frontal face generation, which consistently show the advantage of our new method.

**Keywords:** Face Generation · Attribute · GAN.

## 1 Introduction

This paper proposes a practical approach, *attribute-guided face generation*, for natural face image generation where facial appearance can be easily controlled by user-supplied attributes. Figure 1 shows that by simply providing a high-res image of Ivanka Trump, our face superresolution result preserves her identity which is not necessarily guaranteed by conventional face superresolution (Figure 1: top row). When the input attribute/identity image is a different person, our method transfers the man’s identity to the high-res result, where the low-res input is originally downsampled from a woman’s face (Figure 1: bottom row).

---

\* This work was partially done when Yongyi Lu was an intern at Tencent Youtu.

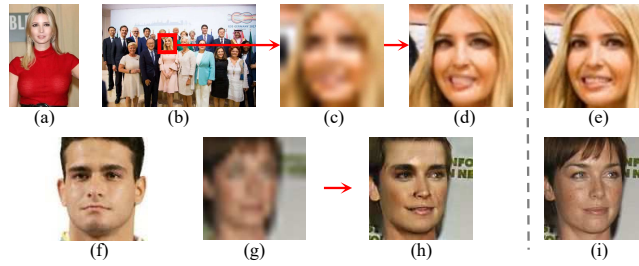


**Fig. 1.** Identity-guided face generation. Top: identity-preserving face super-resolution where (a) is the identity image; (b) input photo; (c) image crop from (b) in low resolution; (d) our generated high-res result; (e) ground truth image. Bottom: face transfer, where (f) is the identity image; (g) input low-res image of another person provides overall shape constraint; (h) our generated high-res result where the man’s identity is transferred. To produce the low-res input (g) we down-sample from (i), which is a woman’s face.

We propose to address our face generation problem using conditional CycleGAN. The original unconditional CycleGAN [23], where enforcing cycle consistency has demonstrated state-of-the-art results in photographic image synthesis, was designed to handle unpaired training data. Relaxing the requirement of paired training data is particularly suitable in our case because the training low/high-res and high-res attribute images do not need to align with each other. By enforcing cycle consistency, we are able to learn a bijective mapping, or one-to-one correspondence with unpaired data from the same/different domains. By simply altering the attribute condition, our approach can be directly applied to generate high-quality face images that simultaneously preserve the constraints given in the low-res input while transferring facial features (e.g., gender, hair color, emotion, sun-glasses) prescribed by input face attributes.

Founded on CycleGAN, we present significant results on both attribute-guided and identity-guided face generation, which we believe is important and timely. Technically, our contribution consists of the new conditional CycleGAN to guide the single-image super-resolution process via the embedding of complex attributes for generating images with high level of photo-realism:

First, in our *attribute-guided conditional CycleGAN*, the adversarial loss is modified to include a conditional feature vector as part of the input to the generator and intra layer to the discriminator as well. Using the trained network we demonstrate impressive results including gender change, transfer of hair color and facial emotion.

Second, in our *identity-guided conditional CycleGAN*, we incorporate a face verification network to produce the conditional vector, and define the proposed identity loss in an auxiliary discriminator for preserving facial identity. Using the trained network, we demonstrate realistic results on identity transfer which are robust to pose variations and partial occlusion. We demonstrate three ap-

plications of identity-guided conditional CycleGAN: identity-preserving face super-resolution, face swapping, and frontal face generation.

## 2 Related Work

Recent state-of-the-art image generation techniques have leveraged the deep convolutional neural networks (CNNs). For example, in single-image superresolution (SISR), a deep recursive CNN for SISR was proposed in [8]. Learning upscaling filters have improved accuracy and speed [3, 16, 17]. A deep CNN approach was proposed in [2] using bicubic interpolation. The ESPCN [16] performs SR by replacing the deconvolution layer in lieu of upscaling layer. However, many existing CNN-based networks still generate blurry images. The SRGAN [10] uses the Euclidean distance between the feature maps extracted from the VGGNet to replace the MSE loss which cannot preserve texture details. The SRGAN has improved the perceptual quality of generated SR images. A deep residual network (ResNet) was proposed in [10] that produces good results for upscaling factors up to 4. In [7] both the perceptual/feature loss and pixel loss are used in training SISR.

Existing GANs [4, 1, 21] have generated state-of-the-art results for automatic image generation. The key of their success lies in the adversarial loss which forces the generated images to be indistinguishable from real images. This is achieved by two competing neural networks, the generator and the discriminator. In particular, the DCGAN [14] incorporates deep convolutional neural networks into GANs, and has generated some of the most impressive realistic images to date. GANs are however notoriously difficult to train: GANs are formulated as a minimax “game” between two networks. In practice, it is hard to keep the generator and discriminator in balance, where the optimization can oscillate between solutions which may easily cause the generator to collapse. Among different techniques, the conditional GAN [6] addresses this problem by enforcing forward-backward consistency, which has emerged to be one of the most effective ways to train GAN.

Forward-backward consistency has been enforced in computer vision algorithms such as image registration, shape matching, co-segmentation, to name a few. In the realm of image generation using deep learning, using unpaired training data, the CycleGAN [23] was proposed to learn image-to-image translation from a source domain  $X$  to a target domain  $Y$ . In addition to the standard GAN loss respectively for  $X$  and  $Y$ , a pair of cycle consistency losses (forward and backward) was formulated using L1 reconstruction loss. Similar ideas can also be found in [9, 20]. For forward cycle consistency, given  $x \in X$  the image translation cycle should reproduce  $x$ . Backward cycle consistency is similar. In this paper, we propose conditional CycleGAN for face image generation so that the image generation process can preserve (or transfer) facial identity, where the results can be controlled by various input attributes. Preserving facial identity has also been explored in synthesizing the corresponding frontal face image from a single side-view face image [5], where the identity preserving loss was defined

based on the activations of the last two layers of the Light CNN [19]. In multi-view image generation from a single view [22], a condition image (e.g. frontal view) was used to constrain the generated multiple views in their coarse-to-fine framework. However, facial identity was not explicitly preserved in their results and thus many of the generated faces look smeared, although as the first generated results of multiple views from single images, the pertinent results already look quite impressive.

While our conditional CycleGAN is an image-to-image translation framework, [13] factorizes an input image into a latent representation  $z$  and conditional information  $y$  using their respective trained encoders. By changing  $y$  into  $y'$ , the generator network then combines the same  $z$  and new  $y'$  to generate an image that satisfies the new constraints encoded in  $y'$ . We are inspired by their best conditional positioning, that is, where  $y'$  should be concatenated among all of the convolutional layers. For SISR, in addition,  $z$  should represent the embedding for a (unconstrained) high-res image, where the generator can combine with the identity feature  $y$  to generate the super-resolved result. In [11] the authors proposed to learn the dense correspondence between a pair of input source and reference, so that visual attributes can be swapped or transferred between them. In our identity-guided conditional CycleGAN, the input reference is encoded as a conditional identity feature so that the input source can be transformed to target identity even though they do not have perceptually similar structure.

### 3 Conditional CycleGAN

#### 3.1 CycleGAN

A Generative Adversarial Network [4] (GAN) consists of two neural networks, a generator  $G_{X \rightarrow Y}$  and a discriminator  $D_Y$ , which are iteratively trained in a two-player minimax game manner. The adversarial loss  $\mathcal{L}(G_{X \rightarrow Y}, D_Y)$  is defined as

$$\begin{aligned} \mathcal{L}(G_{X \rightarrow Y}, D_Y) = \min_{\Theta_g} \max_{\Theta_d} \{ & \mathbb{E}_y[\log D_Y(y)] \\ & + \mathbb{E}_x[\log(1 - D_Y(G_{X \rightarrow Y}(x)))] \} \end{aligned} \quad (1)$$

where  $\Theta_g$  and  $\Theta_d$  are respectively the parameters of the generator  $G_{X \rightarrow Y}$  and discriminator  $D_Y$ , and  $x \in X$  and  $y \in Y$  denotes the *unpaired* training data in source and target domain respectively.  $\mathcal{L}(G_{Y \rightarrow X}, D_X)$  is analogously defined.

In CycleGAN,  $X$  and  $Y$  are two different image representations, and the CycleGAN learns the translation  $X \rightarrow Y$  and  $Y \rightarrow X$  simultaneously. Different from “pix2pix” [6], training data in CycleGAN is unpaired. Thus, they introduce Cycle Consistency to enforce forward-backward consistency which can be considered as “pseudo” pairs of training data. With the Cycle Consistency, the loss function of CycleGAN is defined as:

$$\begin{aligned} \mathcal{L}(G_{X \rightarrow Y}, G_{Y \rightarrow X}, D_X, D_Y) = & \mathcal{L}(G_{X \rightarrow Y}, D_Y) \\ & + \mathcal{L}(G_{Y \rightarrow X}, D_X) + \lambda \mathcal{L}_c(G_{X \rightarrow Y}, G_{Y \rightarrow X}) \end{aligned} \quad (2)$$

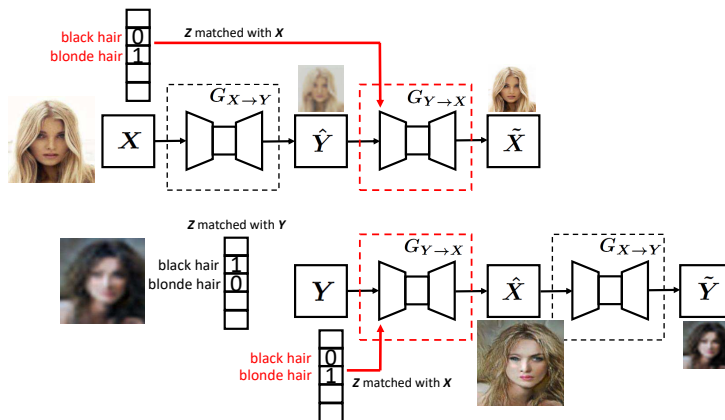


**Fig. 2.** Our Conditional CycleGAN for attribute-guided face generation. In contrast to the original CycleGAN, we embed an additional attribute vector  $z$  (e.g., blonde hair) which is associated with the input attribute image  $X$  to train a generator  $G_{Y \rightarrow X}$  as well as the original  $G_{X \rightarrow Y}$  to generate high-res face image  $\tilde{X}$  given the low-res input  $Y$  and the attribute vector  $z$ . Note the discriminators  $D_X$  and  $D_Y$  are not shown for simplicity.

where

$$\begin{aligned} \mathcal{L}_c(G_{X \rightarrow Y}, G_{Y \rightarrow X}) = & \|G_{Y \rightarrow X}(G_{X \rightarrow Y}(x)) - x\|_1 \\ & + \|G_{X \rightarrow Y}(G_{Y \rightarrow X}(y)) - y\|_1 \end{aligned} \quad (3)$$

is the Cycle Consistency Loss. In our implementation, we adopt the network architecture of CycleGAN to train our conditional CycleGAN with the technical contributions described in the next subsections.

### 3.2 Attribute-guided Conditional CycleGAN

We are interested in natural face image generation guided by user-supplied facial attributes to control the high-res results. To include conditional constraint into the CycleGAN network, the adversarial loss is modified to include the conditional feature vector  $z$  as part of the input of the generator and intra layer to the discriminator as

$$\begin{aligned} \mathcal{L}(G_{(X,Z) \rightarrow Y}, D_Y) = & \min_{\Theta_g} \max_{\Theta_d} \{ \mathbb{E}_{y,z} [\log D_Y(y, z)] \\ & + \mathbb{E}_{x,z} [\log(1 - D_Y(G_{(X,Z) \rightarrow Y}(x, z), z))] \} \end{aligned} \quad (4)$$

$\mathcal{L}(G_{(Y,Z) \rightarrow X}, D_X)$  is defined analogously.

With the conditional adversarial loss, we modify the CycleGAN network as illustrated in Figure 2. We follow [13] to pick 18 attributes as our conditional feature vector. Note that in our conditional CycleGAN, the attribute vector is

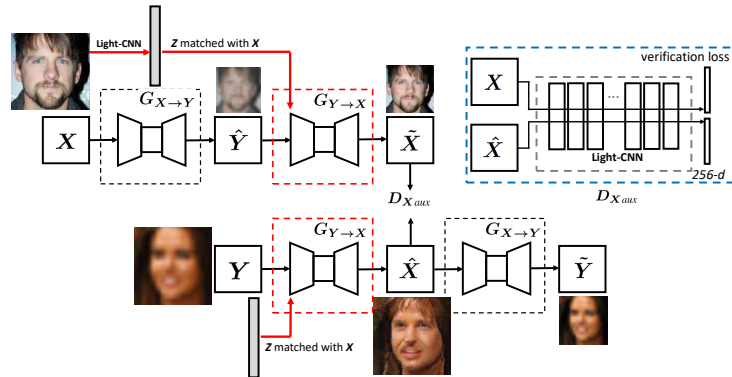


**Fig. 3.** Our Conditional CycleGAN for identity-guided face generation. Different from attribute-guided face generation, we incorporate a face verification network as both the source of conditional vector  $z$  and the proposed identity loss in an auxiliary discriminator  $D_{X_{aux}}$ . The network  $D_{X_{aux}}$  is pre-trained. Note the discriminators  $D_X$  and  $D_Y$  are not shown for simplicity.

associated with the input high-res face image (i.e.,  $X$ ), instead of the input low-res face image (i.e.,  $Y$ ). In each “pair” of training iteration, the same conditional feature vector is used to generate the high-res face image (i.e.,  $\hat{X}$ ). Hence, the generated intermediate high-res face image in the lower branch of Figure 2 will have different attributes from the corresponding ground truth high-res image. This is on purpose because the conditional discriminator network would enforce the generator network to utilize the information from the conditional feature vector. If the conditional feature vector always receives the correct attributes, the generator network would learn to skip the information in the conditional feature vector, since some of the attributes can be found in the low-res face image.

In our implementation, the conditional feature vector is first replicated to match the size of the input image which is downsampled into a low-res. Hence, for  $128 \times 128$  low-res input and 18-dimensional feature vector, we have  $18 \times 128 \times 128$  homogeneous feature maps after resizing. The resized feature is then concatenated with the *input* layer of the generator network to form a  $(18 + 3) \times 128 \times 128$  tensor to propagate the inference of feature vector to the generated images. In the discriminator network, the resized feature (with size  $18 \times 64 \times 64$ ) is concatenated with the *conv1* layer to form a  $(18 + 64) \times 64 \times 64$  tensor.

Algorithm 1 describes the the whole training procedure, with the network illustrated in Figure 2. In order to train the conditional GAN network, only the correct pair of groundtruth high-res face image and the associated attribute feature vector are treated as positive examples. The generated high-res face image with the associated attribute feature vector, and the groundtruth high-res face image with randomly sampled attribute feature vector are both treated

---

**Algorithm 1** Conditional CycleGAN training procedure (using minibatch SGD as illustration)

---

**Input:** Minibatch image sets  $x \in X$  and  $y \in Y$  in target and source domain respectively, attribute vectors  $z$  matched with  $x$  and mismatching  $\hat{z}$ , number of training batch iterations  $S$

**Output:** Update generator and discriminator weights  $\theta_{g(X \rightarrow Y)}$ ,  $\theta_{g(Y \rightarrow X)}$ ,  $\theta_{d(X)}$ ,  $\theta_{d(Y)}$

- 1:  $\theta_{g(X \rightarrow Y)}$ ,  $\theta_{g(Y \rightarrow X)}$ ,  $\theta_{d(X)}$ ,  $\theta_{d(Y)}$   $\leftarrow$  initialize network parameters
  - 2: **for**  $n = 1$  to  $S$  **do**
  - 3:  $\hat{y} \leftarrow G_{X \rightarrow Y}(x)$  {Forward cycle  $X \rightarrow Y$ , fake  $\hat{y}$ }
  - 4:  $\tilde{x} \leftarrow G_{Y \rightarrow X}(\hat{y}, z)$  {Forward cycle  $Y \rightarrow X$ , reconstructed  $\tilde{x}$ }
  - 5:  $\hat{x} \leftarrow G_{Y \rightarrow X}(y, z)$  {Backward cycle  $Y \rightarrow X$ , fake  $\hat{x}$ }
  - 6:  $\tilde{y} \leftarrow G_{X \rightarrow Y}(\hat{x})$  {Backward cycle  $X \rightarrow Y$ , reconstructed  $\tilde{y}$ }
  - 7:  $\rho_r \leftarrow D_Y(y)$  {Compute  $D_Y$ , real image}
  - 8:  $\rho_f \leftarrow D_Y(\hat{y})$  {Compute  $D_Y$ , fake image}
  - 9:  $s_r \leftarrow D_X(y, z)$  {Compute  $D_X$ , real image, right attribute}
  - 10:  $s_f \leftarrow D_X(\hat{y}, z)$  {Compute  $D_X$ , fake image, right attribute}
  - 11:  $s_w \leftarrow D_X(y, \hat{z})$  {Compute  $D_X$ , real image, wrong attribute}
  - 12:  $\mathcal{L}_{D_Y} \leftarrow \log(\rho_r) + \log(1 - \rho_f)$  {Compute  $D_Y$  loss}
  - 13:  $\theta_{d(Y)} \leftarrow \theta_{d(Y)} - \alpha \nabla_{\theta_{d(Y)}} \mathcal{L}_{D_Y}$  {Update on  $D_Y$ }
  - 14:  $\mathcal{L}_{D_X} \leftarrow \log(s_r) + [\log(1 - s_f) + \log(1 - s_w)] / 2$   
{Compute  $D_X$  loss}
  - 15:  $\theta_{d(X)} \leftarrow \theta_{d(X)} - \alpha \nabla_{\theta_{d(X)}} \mathcal{L}_{D_X}$  {Update on  $D_X$ }
  - 16:  $\mathcal{L}_c = \lambda_1 \|\tilde{x} - x\|_1 + \lambda_2 \|\tilde{y} - y\|_1$  {Cycle consistency loss}
  - 17:  $\mathcal{L}_{G_{X \rightarrow Y}} \leftarrow \log(\rho_f) + \mathcal{L}_c$  {Compute  $G_{X \rightarrow Y}$  loss}
  - 18:  $\theta_{g(X \rightarrow Y)} \leftarrow \theta_{g(X \rightarrow Y)} - \alpha \nabla_{\theta_{g(X \rightarrow Y)}} \mathcal{L}_{G_{X \rightarrow Y}}$   
{Update on  $G_{X \rightarrow Y}$ }
  - 19:  $\mathcal{L}_{G_{Y \rightarrow X}} \leftarrow \log(s_f) + \mathcal{L}_c$  {Compute  $G_{Y \rightarrow X}$  loss}
  - 20:  $\theta_{g(Y \rightarrow X)} \leftarrow \theta_{g(Y \rightarrow X)} - \alpha \nabla_{\theta_{g(Y \rightarrow X)}} \mathcal{L}_{G_{Y \rightarrow X}}$   
{Update on  $G_{Y \rightarrow X}$ }
  - 21: **end for**
- 

as negative examples. In contrast to traditional CycleGAN, we use conditional adversarial loss and conditional cycle consistency loss for updating the networks.

### 3.3 Identity-guided Conditional CycleGAN

To demonstrate the efficacy of our conditional CycleGAN guided by control attributes, we specialize it into identity-guided face image generation. We utilize the feature vector from a face verification network, i.e. Light-CNN [19] as the conditional feature vector. The identity feature vector is a 256-D vector from the ‘‘Light CNN-9 model’’. Compared with another state-of-the-art FaceNet [15], which returns a 1792-D face feature vector for each face image, the 256-D representation of light-CNN obtains state-of-the-art results while it has fewer parameters and runs faster. Though among the best single models, the Light-CNN can be easily replaced by other face verification networks like FaceNet or VGG-Face.

**Auxiliary Discriminator** In our initial implementation, we follow the same architecture and training strategy to train the conditional CycleGAN for identity-guided face generation. However, we found that the trained network does not generate good results (sample shown in Figure 12 (d)). We believe this is because the discriminator network is trained from scratch, and the trained discriminator network is not as powerful as the light-CNN which was trained from million pairs of face images.

Thus, we add an auxiliary discriminator  $D_{X_{aux}}$  on top of the conditional generator  $G_{Y \rightarrow X}$  in parallel with the discriminator network  $D_X$  so there are two discriminators for  $G_{Y \rightarrow X}$ , while the discriminator for  $G_{X \rightarrow Y}$  remains the same (as illustrated in Figure 3). Our auxiliary discriminator takes an input of the generated high-res image  $\hat{X}$  or the ground truth image  $X$ , and outputs a feature embedding. We reuse the pretrained Light-CNN model for our auxiliary discriminator, the activation of the second last layer: the 256-D vector same as our conditional vector  $Z$ .

Based on the output of the auxiliary discriminator, we define an identity loss to better guide the learning of the generator. Here we use the L1 loss of the output 256-D vectors as our identity loss. The verification errors from the auxiliary discriminator is back propagated concurrently with the errors from the discriminator network. With the face verification loss, we are able to generate high quality high-res face images matching the identity given by the conditional feature vector. As shown in the running example in Figure 3, the lady’s face is changed to a man’s face whose identify is given by the light-CNN feature.

## 4 Experiments

We use two image datasets, MNIST (for sanity check) and CelebA [12] (for face image generation) to evaluate our method. The MNIST is a digit dataset of 60,000 training and 10,000 testing images. Each image is a  $28 \times 28$  black and white digit image with the class label from 0 to 9. The CelebA is a face dataset of 202,599 face images, with 40 different attribute labels where each label is a binary value. We use the aligned and cropped version, with 182K images for training and 20K for testing. To generate low-res images, we downsampled the images in both datasets by a factor of 8, and we separate the images such that the high-res and low-res training images are non-overlapping.

### 4.1 MNIST

We first evaluate the performance of our method on MNIST dataset. The conditional feature vector is the class label of digits. As shown in Figure 4, our method can generate high-res digit images from the low-res inputs. Note that the generated high-res digit follows the given class label when there is conflict between the low-res image and feature vector. This is desirable, since the conditional constraint consumes large weights during the training. This sanity check also verifies that we can impose conditional constraint into the CycleGAN network.

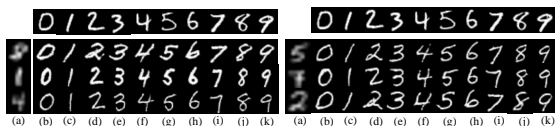


**Fig. 4.** From the low-res digit images (a), we can generate high-res digit images (b) to (k) subject to the conditional constrain from the digit class label in the first row.

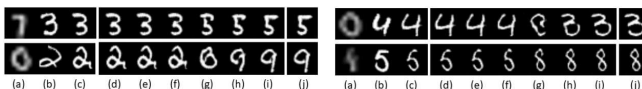


**Fig. 5.** Interpolation results of digits. Given the low-res inputs in (a), we randomly sample two digits (b) and (j). (c) is the generated results from (a) conditioned on the attribute of (b). Corresponding results of interpolating between attributes of (b) and (j) are shown in (d) to (i). We interpolate between the binary vectors of the digits.

In addition to the label changes based on the high-res identity inputs, we observe that the generated high-res images inherit the appearance in the low-res inputs such as the orientation and thickness. For the ‘8’ example in Figure 4 the outputs share the same slanting orientation with the low-res ‘8’ which is tilted to the right. In the next row the outputs adopt the thickness of the input, that is, the relatively thick stroke presented by the low-res ‘1’. This is a good indicator of the ability of our trained generator: freedom in changing labels based on the high-res images presented as identity attribute, while preserving the essential appearance feature presented by the low-res inputs.

Apart from generating high-res digit images from the low-res inputs, we also perform linear interpolation between two high-res images (as identity features) to show our model is able to learn the digit representation. Specifically, we interpolate between the respective binary vectors of the two digits. Sample results are shown in Figure 5.

## 4.2 Attribute-guided Face Generation

Figure 6 shows sample results for attribute guided face generation. Recall the condition is encoded as a 18-D vector. The 10 results shown in the figure are generated with one attribute label flipped in their corresponding condition vector in conditional CycleGAN. Our generated results conditioned on attributes such as BANGS, BLOND\_HAIR, BUSHY\_EYEBROWS, GENDER, PALE\_SKIN are quite convincing.

**Comparison with Conditional GAN.** We first compare with conditional GAN framework [13] under the attribute-guided face generation framework. Visualizations are shown in Figure 7. Generally, our method can generate much



**Fig. 6.** Attribute-guided face generation. We flip one attribute label for each generated high-res face images, given the low-res face inputs. The 10 labels are: Bald, Bangs, Blond\_Hair, Gray\_Hair, Bushy\_Eyebrows, Eyeglasses, Male, Pale\_Skin, Smiling, Wearing\_Hat.



**Fig. 7.** Comparison with [13] by swapping facial attributes. Four paired examples are shown. Generally, our method can generate much better images compared to [13].

better images compared to the competitor, e.g., our methods successfully removes the eyeglasses, as well as generates the right color of hairs. Note that [13] generates different persons while ours are faithful to the inputs.

**Comparison with Unsupervised GAN.** We further compare with [9], which is also a unpaired image-to-image translation method. Comparison results are shown in Figure 8. Note we only provide part of the attribute results according to their paper for fair comparison.

**Quantitative Comparison.** To quantitatively evaluate the generated results, we use structural similarity (SSIM) [18], which is a widely used image quality metric that correlates well with human visual perception. SSIM ranges from 0 to 1, higher is better. The SSIM of our method, as well as conditional GAN [13] and unsupervised GAN [9], is shown in Table 1 for the generated images.

Our method outperforms [13] and [9] in two aspects: (i) In the unsupervised GAN setting, compared with [9], our method shows significant performance gain



**Fig. 8.** Comparison results with [9]. Four source images are shown in top row. Images with blue and red bounding boxes indicates transferred results by [9] and results by our method, respectively.

**Table 1.** SSIM on CelebA test sets.

Method	Conditional GAN [13]	Unsupervised GAN [9]	Conditional CycleGAN
SSIM	0.74	0.87	<b>0.92</b>

with the proposed attributed guided framework. (ii) compared with conditional GAN [13], the performance gain is even larger with the help of the cyclic network architecture of our conditional CycleGAN.

### 4.3 Identity-guided Face Generation

Figure 9 and Figure 10 show sample face generation results where the identity face features are respectively from the same and *different* persons. There are two interesting points to note: First, the generated high-res results (c) bear high resemblance to the target identity images (b) from which the identity features are computed using Light-CNN. The unique identity features transfer well from (b) to (c), e.g., challenging gender change in the second row of Figure 10. In the last row, the facial attributes, e.g. beard (example in the blue box), eyeglasses (example in the yellow box) are considered as parts of the identity and faithfully preserved by our model in the high-res outputs, even though the low-res inputs do not have such attributes. The occluded forehead in low-res input (example in the green box) is recovered. Second, the low-res inputs provide overall shape constraint. The head pose and facial expression of the generated high-res images (c) adopt those in the *low-res* inputs (a). Specifically, refer to the example inside the blue box in the last row of Figure 10, where (b) shows target identity, i.e. man smiling while low-res input (a) shows another man with closed mouth. The generated high-res image in (c) preserves the identity in (b) while the pose of the head follows the input and the mouth is closed as well.

### 4.4 Face Swapping within the High-Res Domain

We demonstrate an interesting application *face swapping* where *both* the input and identity images are high-res images. Here, we want to swap the identity

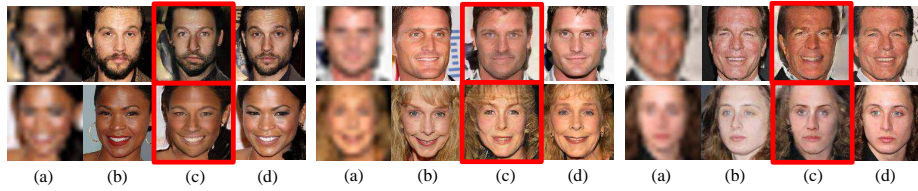


**Fig. 9.** Identity-guided face generation results on low-res input and high-res identity of the same person, i.e., identity-preserving face superresolution. (a) low-res inputs; (b) input identity of the same person; (c) our high-res face outputs (red boxes) from (a); (d) the high-res ground truth of (a).

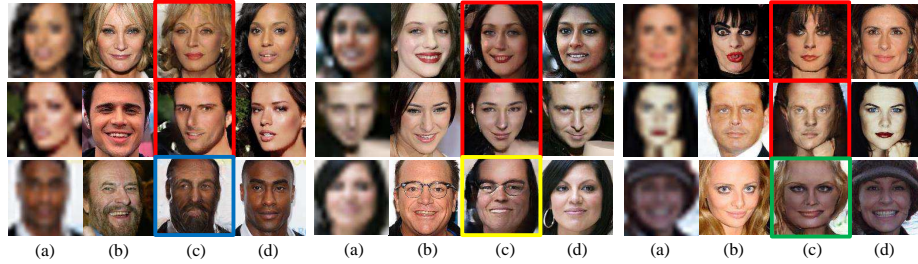


**Fig. 10.** Identity-guided face generation results on different persons. The last row shows some challenging examples, e.g., the occluded forehead in low-res input is recovered (example in the green box). (a) low-res inputs provide overall shape constraint; (b) identity to be transferred; (c) our high-res face outputs (red boxes) from (a) where the man/woman’s identity in (b) is transferred; (d) the high-res ground truth of (a).

while preserving *all* facial details including subtle crease lines and expression, thus both the identity image and the input image must be high-res images. We adopt our identity-guided conditional CycleGAN and utilize Light-CNN as both the source of the identity features and face verification loss. Our face swapping results are shown in Figure 11. As illustrated, our method swaps the identity by transferring the appearance of eyes, eyebrows, hairs, etc, while keeping other factors intact, e.g., head pose, shape of face and facial expression. Without multiple steps (e.g., facial landmark detection followed by warping and blending) in traditional techniques, our identity-guided conditional CycleGAN can still achieve high levels of photorealism of the face-swapped images.

Figure 12 compares face swapping results of our models trained with and without the face verification loss in the auxiliary discriminator. The difference is easy to recognize, and adding face verification loss has a perceptual effect of improving the photorealism of swapped-face image. In this example, the eyebrows and eyes are successfully transformed to the target identity with the face verification loss.

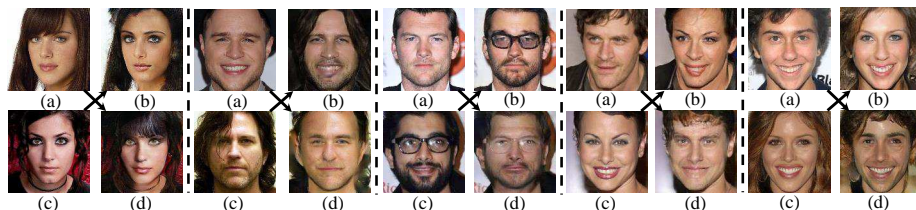


**Fig. 11.** Face swapping results within the high-res domain. (a)(c) are inputs of two different persons; (b)(d) their face swapping results. The black arrows indicate the guidance of identity, i.e. (d) is transformed from (c) under the identity constraint of (a). Similarly, (b) is transformed from (a) under the identity of (c). Note how our method transforms the identity by altering the appearance of eyes, eyebrows, hairs etc, while keeping other factors intact, e.g., head pose, shape of face and facial expression.

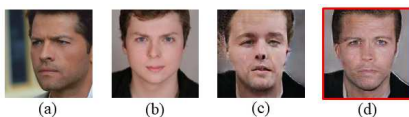


**Fig. 12.** Results without (c) and with (d) face verification loss. (a) is target identity image to be transferred and (b) is input image. The loss encourages subtle yet important improvement in photorealism, e.g. the eyebrows and eyes in (c) resemble the target identity in (a) by adding the face verification loss.

#### 4.5 Frontal Face Generation

Another application of our model consists of generating images of frontal faces from face images in other orientations. By simply providing a low-res frontal face image and adopting our identity-guided conditional CycleGAN model, we can generate the corresponding high-res frontal face images given side-face images as high-res face attributes. Figure 13 shows sample results on our frontal face image generation. Note that our frontal face generation is end-to-end and free of human intervention, thus setting it apart from related works of frontalizing the face by landmark detection, warping and blending etc. given a frontal pose.

#### 4.6 Interpolating Conditional Vector

We further explore the conditional attribute vector by linearly interpolating between two different attribute vectors. Figure 14 shows that all the interpolated faces are visually plausible with smooth transition among them, which is a convincing demonstration that the model generalizes well the face representation instead of just directly memorizes the training samples.

Similar to interpolating the attribute vectors, we experiment with interpolating the 256-D identity feature vectors under our identity-guided conditional

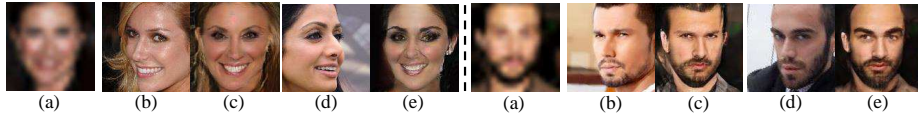


**Fig. 13.** Frontal face generation. Given a low-res template (a), our method can generate corresponding frontal faces from different side faces, e.g., (b) to (c), (d) to (e).

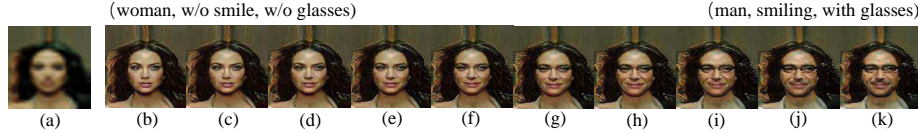


**Fig. 14.** Interpolation results of the attribute vectors. (a) Low-res face input; (b) generated high-res face images; (c) to (k) interpolated results. Attributes of source and destination are shown in text.

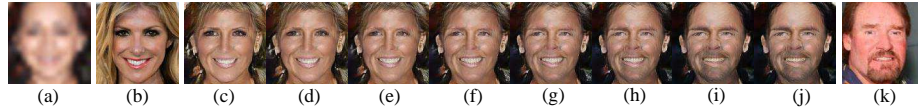


**Fig. 15.** Interpolating results of the identity feature vectors. Given the low-res input in (a), we randomly sample two target identity face images (b) and (k). (c) is the generated face from (a) conditioned on the identity in (b) and (d) to (j) are interpolations.

model. We randomly sample two high-res face images and interpolate between the two identity features. Figure 15 indicates that our model generalizes properly the face representation given the conditional feature vectors.

## 5 Conclusion

We have presented the Conditional CycleGAN for attribute-guided and identity-guided face image generation. Our technical contribution consists of the conditional CycleGAN to guide the face image generation process via easy user input of complex attributes for generating high quality results. In the attribute-guided conditional CycleGAN, the adversarial loss is modified to include a conditional feature vector as parts of the inputs to the generator and discriminator networks. We utilize the feature vector from light-CNN in identity-guided conditional CycleGAN. We have presented the first but significant results on identity-guided and attribute-guided face image generation. In the future, we will explore how to further improve the results and extend the work to face video generation.

**Acknowledgement** This work was supported in part by Tencent Youtu.

## References

1. Choi, Y., Choi, M., Kim, M., Ha, J.W., Kim, S., Choo, J.: Stargan: Unified generative adversarial networks for multi-domain image-to-image translation. In: The IEEE Conference on Computer Vision and Pattern Recognition (CVPR) (June 2018)
2. Dong, C., Loy, C.C., He, K., Tang, X.: Learning a Deep Convolutional Network for Image Super-Resolution (2014)
3. Dong, C., Loy, C.C., Tang, X.: Accelerating the super-resolution convolutional neural network. CoRR **abs/1608.00367** (2016), <http://arxiv.org/abs/1608.00367>
4. Goodfellow, I., Pouget-Abadie, J., Mirza, M., Xu, B., Warde-Farley, D., Ozair, S., Courville, A., Bengio, Y.: Generative adversarial nets. In: NIPS, pp. 2672–2680 (2014), <http://papers.nips.cc/paper/5423-generative-adversarial-nets.pdf>
5. Huang, R., Zhang, S., Li, T., He, R.: Beyond Face Rotation: Global and Local Perception GAN for Photorealistic and Identity Preserving Frontal View Synthesis. ArXiv e-prints (Apr 2017)
6. Isola, P., Zhu, J., Zhou, T., Efros, A.A.: Image-to-image translation with conditional adversarial networks. CoRR **abs/1611.07004** (2016), <http://arxiv.org/abs/1611.07004>
7. Johnson, J., Alahi, A., Li, F.: Perceptual losses for real-time style transfer and super-resolution. CoRR **abs/1603.08155** (2016), <http://arxiv.org/abs/1603.08155>
8. Kim, J., Lee, J.K., Lee, K.M.: Deeply-recursive convolutional network for image super-resolution. In: CVPR. pp. 1637–1645 (2016)
9. Kim, T., Cha, M., Kim, H., Lee, J., Kim, J.: Learning to discover cross-domain relations with generative adversarial networks. ICML (2017)
10. Ledig, C., Theis, L., Huszar, F., Caballero, J., Aitken, A.P., Tejani, A., Totz, J., Wang, Z., Shi, W.: Photo-realistic single image super-resolution using a generative adversarial network. CoRR **abs/1609.04802** (2016), <http://arxiv.org/abs/1609.04802>
11. Liao, J., Yao, Y., Yuan, L., Hua, G., Kang, S.B.: Visual Attribute Transfer through Deep Image Analogy. SIGGRAPH (2017)
12. Liu, Z., Luo, P., Wang, X., Tang, X.: Deep learning face attributes in the wild. CoRR **abs/1411.7766** (2014)
13. Perarnau, G., van de Weijer, J., Raducanu, B., Álvarez, J.M.: Invertible Conditional GANs for image editing. In: NIPS Workshop on Adversarial Training (2016)
14. Radford, A., Metz, L., Chintala, S.: Unsupervised representation learning with deep convolutional generative adversarial networks. CoRR **abs/1511.06434** (2015), <http://arxiv.org/abs/1511.06434>
15. Schroff, F., Kalenichenko, D., Philbin, J.: Facenet: A unified embedding for face recognition and clustering. In: CVPR (June 2015)
16. Shi, W., Caballero, J., Huszar, F., Totz, J., Aitken, A.P., Bishop, R., Rueckert, D., Wang, Z.: Real-time single image and video super-resolution using an efficient sub-pixel convolutional neural network. In: CVPR. pp. 1874–1883 (2016)
17. Wang, Y., Wang, L., Wang, H., Li, P.: End-to-end image super-resolution via deep and shallow convolutional networks. CoRR **abs/1607.07680** (2016), <http://arxiv.org/abs/1607.07680>
18. Wang, Z., Bovik, A.C., Sheikh, H.R., Simoncelli, E.P.: Image quality assessment: from error visibility to structural similarity. IEEE transactions on image processing **13**(4), 600–612 (2004)

19. Wu, X., He, R., Sun, Z.: A lightened CNN for deep face representation. CoRR **abs/1511.02683** (2015), <http://arxiv.org/abs/1511.02683>
20. Yi, Z., Zhang, H., Gong, P.T., et al.: Dualgan: Unsupervised dual learning for image-to-image translation. arXiv preprint arXiv:1704.02510 (2017)
21. Zhang, H., Xu, T., Li, H., Zhang, S., Huang, X., Wang, X., Metaxas, D.: Stackgan: Text to photo-realistic image synthesis with stacked generative adversarial networks. In: IEEE Int. Conf. Comput. Vision (ICCV). pp. 5907–5915 (2017)
22. Zhao, B., Wu, X., Cheng, Z.Q., Liu, H., Feng, J.: Multi-View Image Generation from a Single-View. ArXiv e-prints (Apr 2017)
23. Zhu, J.Y., Park, T., Isola, P., Efros, A.A.: Unpaired image-to-image translation using cycle-consistent adversarial networks. In: Computer Vision (ICCV), 2017 IEEE International Conference on (2017)